

# FPGA-Based Hardware in the Loop of MPC-MPPT for New High Step-Up DC/DC Converter

Habib BEY<sup>1</sup>, Fateh KRIM<sup>1</sup>, Moncef KHITAS<sup>1</sup>, Anis KRIM<sup>1</sup>

<sup>1</sup>Power electronics and industrial control laboratory (LEPCI), Department of electronics,

University of Sétif-1, 19000 Sétif, Algeria

E-mail : bey\_habib@univ-setif.dz

**Abstract** - This paper proposes a model predictive control based maximum power point tracking (MPC-MPPT) algorithm with optimum number of sensors for driving high step-up DC/DC converter, in photovoltaic (PV) systems. For utilizing PV module in power generation, the developed controller is designed under MATLAB/Simulink environment; then, field programmable gate array FPGA in the loop (FIL) technique is used to implement the MPC-MPPT model. this digital implementation satisfies the hardware and recommended performance. Which led to a significant increase in processing speed. A computing capability 300 times faster than conventional sequential implementations has been achieved (Parallel computation:  $T_s = 1 \mu s$  with a processing clock of 100 MHz, Sequential computation:  $T_s = 30 \mu s$  with a processing clock of 1 GHz). the experimental validation is carried out on Atlys spartan-6 FPGA Xilinx board using ISE 14.2 processing. MPC is a prevalent control technique with superior transient and steady-state performances in PV systems. The algorithm is designed to operate with both fixed and adaptive step-size. the results obtained confirm proper operation of the developed approach.

**Keywords** - DC/DC converter, Model Predictive Control based Maximum Power Point Tracking (MPC-MPPT), Field Programmable Gate Array (FPGA).

## I. INTRODUCTION

In the domain of PV generation systems, the integration of a DC/DC converter plays a vital role in connecting the low voltage PV panel to the high voltage DC link. This converter is instrumental in ensuring that the full potential of the PV panel is harnessed through the implementation of maximum power point tracking (MPPT) control [1]-[2]. The efficacy of MPPT techniques is commonly assessed based on criteria such as high tracking accuracy, as well as stable transient and steady-state response [3]-[5]. To fulfill these crucial requirements, extensive research has been conducted, exploring various MPPT techniques and their performance characteristics.

One of the classical algorithms employed for MPPT in PV panels is the Perturb and Observe (P&O) algorithm. The P&O algorithm operates by analyzing the slope of the PV curve to identify

and capture the maximum power output of the PV panel. With its widespread usage, the P&O algorithm has proven to be an effective method in harnessing the optimal power generation potential of PV panels [6].

The P&O algorithm suffers from oscillation around the maximum power point (MPP) [7]. Various techniques have been proposed to address this issue and improve MPPT efficiency. For systems that require multivariable control, finite-set model predictive control (FS-MPC) emerges as an appealing solution [8]. The MPC-based MPPT methodology outlined in [9] exhibits efficient tracking of the maximum power of PV modules under various environmental conditions. Nonetheless, it relies on the use of three sensors, comprising two voltage sensors and one current sensor.

In practical scenarios, traditional boost converters cannot achieve an infinite boosting ratio, that's why recently, a new topology, more

efficient than the traditional Boost converter, has been proposed [10]- [11], and it is the subject of our study. This topology is that of a high step-up DC/DC converter, with 2 transistors and 2 freewheeling diodes, in a way, an enhanced Boost converter. This results in a high voltage gain without requiring a large duty cycle.

Speed performance of new components such as FPGAs have already been used with success in many different electric system applications. Including, a power converter control (pulse width-modulation (PWM) inverters) multilevel converters and electrical machines control. This is because an FPGA-based implementation of controllers can efficiently answer current and future challenges of this field. Therefore, hardware in the loop (HIL) methods emerge in system design to be an effective way to exam the performance of electrical systems. HIL methods seem to be an effective alternative to accelerate verification through a specific and relatively low-cost equipment to finally build a real and an operational prototype [12]-[14].

In this work, an effective procedure to design and simulate MPC-MPPT controller for a high step-up DC/DC converter is presented. The hardware description language VHDL has been applied to develop the required blocks for MPC-MPPT controller to offer the advantage of portability for any FPGA, a fixed-point representation of 32 bits in two's complement has been used. The contribution of this work is an effective design way for hardware presentation of MPC-MPPT based on FPGA with a simple description. To prove the performance of the suggested control of MPPT system and to validate the proposed approach, HIL simulations between MATLAB/Simulink and Xilinx 14.2 ISE are investigated.

## II. PHOTOVOLTAIC SYSTEM MODEL

The block diagram of the PV system under consideration is shown in Fig 1. The energy source of the PV system is constituted by a photovoltaic module, the boost converter acts as interface between the solar panel and the load, and the MPPT controller allows reaching the available maximum power. Notice that the

current  $I_{PV}$  and the voltage  $V_{PV}$  provided by the PV module are used as inputs to the Boost converter and to the MPPT controller which is also fed with the output voltage  $v$  of the converter. The average control signal  $u_{av}$  generated by the MPPT controller is sent to the converter.

The proposed MPC-MPPT algorithm does not require an output voltage sensor. The latter is replaced by an observer, which reduces the cost of the system, while ensuring good performance. Another characteristic of the MPC-MPPT technique studied is that the algorithm works with a fixed or adaptive step.

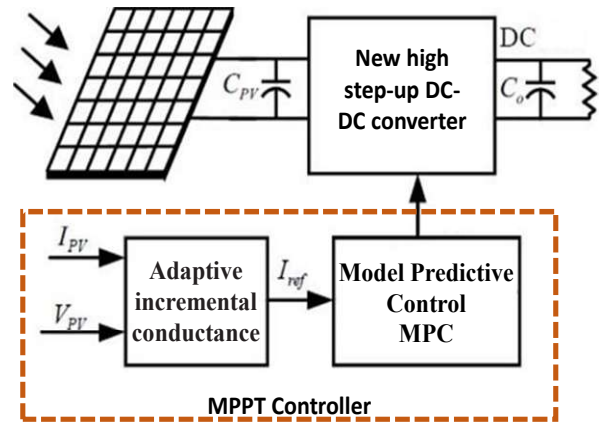


Fig. 1. PV system under a MPPT controller.

## III. HIGH GAIN DC/DC CONVERTER

The topology of the high step-up DC/DC converter is illustrated in Fig 2 [15]. It consists of two inductors ( $L_1$  and  $L_2$ ), three diodes ( $D_1$ ,  $D_2$ , and  $D_3$ ), one output capacitor ( $C_o$ ), and two power switches ( $S_1$  and  $S_2$ ). The converter has two operating modes depending on the switch status,  $S_1=S_2= \{0 \text{ or } 1\}$ , in continuous conduction mode (CCM) or discontinuous conduction mode (DCM).

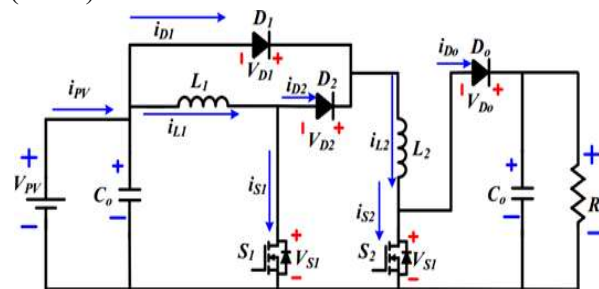


Fig. 2. High step-up DC-DC converter.

### A) MODE I

When the switches are turned on  $S_1=S_2=1$ , diodes  $D_2$  and  $D_0$  are turned off. And hence, inductors  $L_1$  and  $L_2$  are charging from the DC source. The characteristics equations of this mode are as follows:

$$\begin{cases} v_{L1}(t) = V_{PV} \\ i_{PV}(t) = C_{PV} \frac{dV_{PV}}{dt} + 2i_{L1} \\ v_{L2}(t) = V_{PV} \\ C_o \frac{dV_o}{dt} = i_{C_o} = -V_o/R \end{cases} \quad (1)$$

### B) MODE II

When the switches are turned off  $S_1=S_2=0$ , diodes  $D_2$  and  $D_0$  are turned on to provide a path for the inductor currents and diode  $D_1$  is turned off. And hence, inductors  $L_1$  and  $L_2$  are discharging their energy in series to the output capacitor.

The characteristics equations of this mode are as follows:

$$\begin{cases} v_{L1}(t) = v_{L2}(t) = \left( \frac{V_{PV} - V_o}{2} \right) \\ i_{PV}(t) = C_{PV} \frac{dV_{PV}}{dt} + i_{L1} \\ C_o \frac{dV_o}{dt} = i_{C_o} = i_{L1} - V_o/R \end{cases} \quad (2)$$

Applying inductor volt-second balance and capacitor charge-balance leads to

$$\begin{cases} \langle v_{L1}(t) \rangle = 0 \\ \langle v_{L2}(t) \rangle = 0 \\ \langle i_{C_o}(t) \rangle = 0 \end{cases} \quad (3)$$

The relation between output voltage, input voltage, and capacitor can be deduced from (1)-(3).

$$V_o = \left( \frac{1+D}{1-D} \right) V_{PV} \quad (4)$$

Equation (4) is the voltage gain of the converter, where  $D$  is the duty cycle of the converter.

## IV. PROPOSED MPC BASED PV MPPT ALGORITHM

Model Predictive Control offers an effective control strategy for various applications, with particular relevance to systems such as the DC-DC converter. This type of converter typically involves multiple state variables that require precise control. In the context of MPC, the plant is viewed as a collection of distinct linear models, each corresponding to a specific switching state. The MPC algorithm involves predicting the outcomes for each switching state, followed by a minimization process based on a cost function. The selected state with the minimum error is then generated and applied to the plant, as described in references [13] and [14].

In the case of a PV system, the suggested plant is the DC-DC converter. Since it operates in continuous conduction mode, it involves only two state variables. Consequently, a discrete-time model for the proposed DC/DC step-up converter is derived by applying the forward Euler method to two distinct states: (1) switch on and (2) switch off.

$$I_{PV}^1(k+1) = \left( \frac{2T_s}{L_1} \right) V_{PV}(k) + I_{PV}(k) \quad (5)$$

$$I_{PV}^0(k+1) = \left( \frac{T_s}{2L} \right) [V_{PV}(k) - V_o] + I_{PV}(k) \quad (6)$$

The Equations (5) and (6), are predicted PV current if the switch is turned off, and predicted PV current if the switch is turned on, respectively. Three sensors are required to predict the future value of the PV current. This would increase the system cost and size. The Equation (4) is a voltage observer, which is used to calculate the value of the output voltage with the available data of PV voltage and duty cycle. By this methodology, one voltage sensor is removed, which reduces the system cost and at the same time the system performance doesn't affect.

The final step in MPC control is the optimization of the possible future states and select the optimum value that gives the minimum error. Optimization is done by cost function:

$$g^{\sigma=\{0,1\}} = \left| I_{ref} - I_{PV}^{\sigma} \right|, \quad (7)$$

Reference current  $I_{ref}$  is generated by incremental conductance algorithm. The proposed control block is depicted in Fig 3.

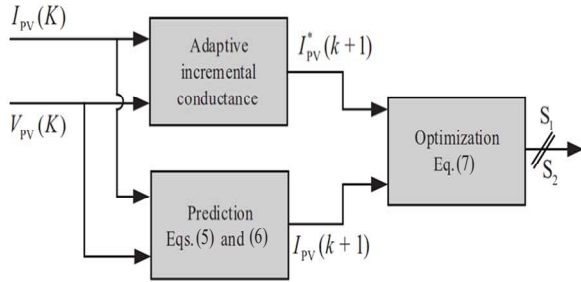


Fig. 3. Control block of the proposed control system.

As illustrated in the fig 3, MPC-MPPT algorithm senses PV current and voltage only, then an incremental conductance approach is applied to generate the reference current that leads to maximum power operation.

The MPC algorithm starts to regulate the converter to track the reference current. The capacitor voltage sensor is omitting by the voltage observer, described in the previous section. The perturbation step size, denoted as  $Z$ , can be set to fixed value to implement a fixed step size MPC-MPPT or it can be designed to be adaptive by the following formula:

(8)

**V. HARDWARE IN THE LOOP IMPLEMENTATION METHOD IN FPGA**

The architecture of the control scheme is depicted in fig 4. The control system includes an adaptative incremental conductance, and MPC controller as present in Fig 5 (a) (b), respectively. All the blocks have been designated using VHDL language, using HDL Coder blocs Toolbox of MATLAB/Simulink, in addition, a pipelined architecture with a register after every operation is apply, to decreases the delay on the combinational logic and maximizes the operating frequency of the architecture.

The complete architecture has been verified using HIL simulations on Xilinx Atlys spartan6 board with a XC6SLX45-3CSG324 FPGA chip. The control is loaded in this case into the FPGA

to implement in real time, whereas the boost converter, and photovoltaic module are simulated using the SimPowerSystems toolbox of MATLAB/ Simulink.

A fixed-point arithmetic has been applied to carry out the hardware description. All variables are determined in two's complement format with a word size of 32 bits dispatched as 1 bit for sign bit, 15 bits for integer word length and 16 bits for fractional word length.

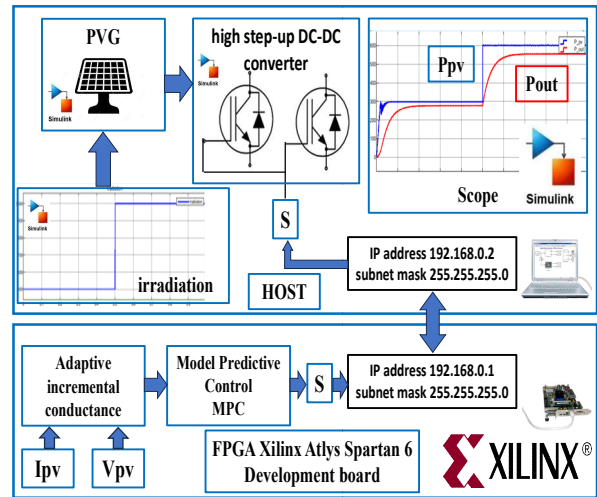
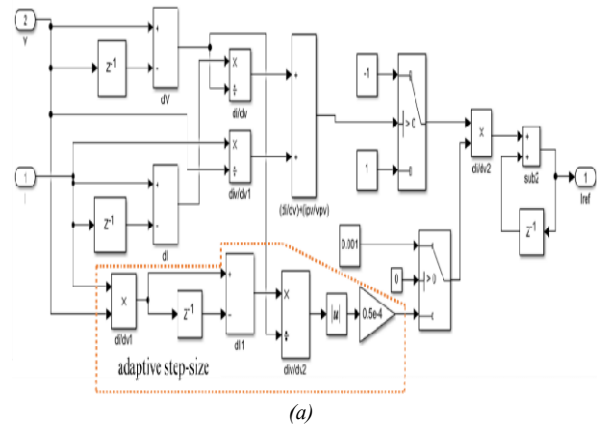
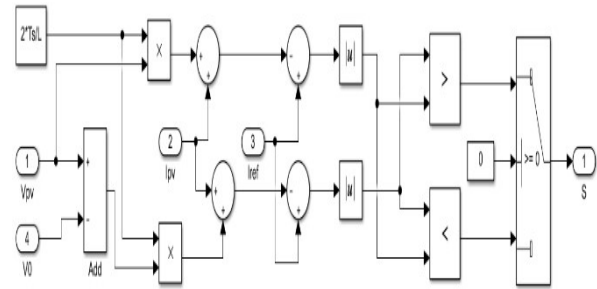


Fig. 4. Block diagram of the photovoltaic chain.



(a)



(b)

Fig. 5. (a) HDL blocks diagram of the incremental method, and (b) HDL blocks diagram of the MPC method.

## VI. EXPERIMENTAL RESULTS

The main progression steps of the MPC-MPPT are illustrated in the flowchart of Fig 6. The fixed-point design is necessary when considering development with FPGA. A balance between performance of architecture and complexity of the hardware to be minimized should be found. Generally, floating-point arithmetic implementations engender nonoptimized use of FPGA resources. In the developed method for fixed-point format determination, fixed-point tools in MATLAB/Simulink are used, while following each data's dynamic range in the control algorithm.

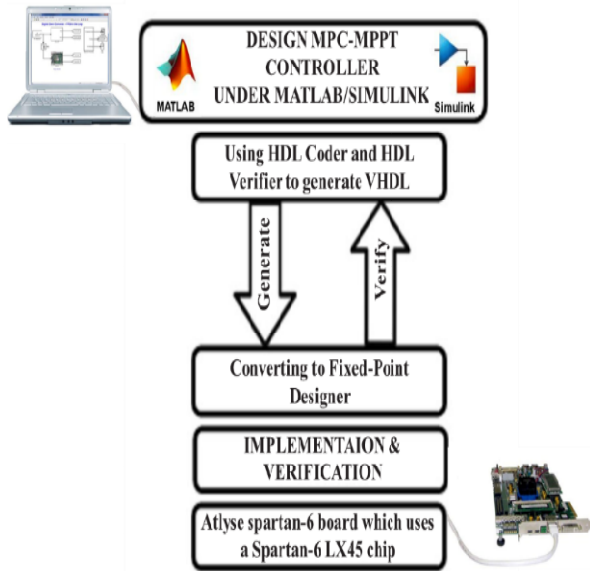


Fig. 6. FPGA in loop co-simulation flowchart.

To validate the MPC-MPPT design, FIL simulations are carried out based on MATLAB/Simulink and Xilinx 14.2 ISE through an Atlyse spartan-6 board which uses a Spartan-6 LX45 chip; this provides the capability to use Simulink software for testing the design in real hardware and in real time. Where the simulation of the electrical part is performed using Simulink while the Xilinx 14.2 ISE software is used to test the hardware architectures. The PV module simulation, and the high step-up DC/DC converter simulation parameters are presented in Table 1 and 2.

TABLE 1. PV MODULE SIMULATION PARAMETERS.

Parameters	Valeur
Open circuit voltage ( $V_{co}$ )	40 V
Voltage at PPM ( $V_{MP}$ )	33.33 V
Short circuit current ( $I_{cc}$ )	4.83 A
Current at PPM ( $I_{mp}$ )	4.51 A
Maximum power	150.3183 W
Temperature coefficient of ( $v_{co}$ )	-0.386 V/°C
Temperature coefficient of ( $I_{cc}$ )	0.043601 %/°C

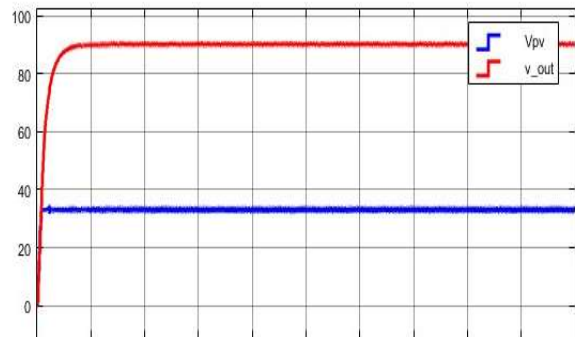
TABLE 2. HIGH STEP-UP DC/DC CONVERTER SIMULATION PARAMETERS.

Parameter / composants	Values /Types
Sampling time	15 $\mu$ s
Inductance ( $L_2$ et $L_1$ )	3 mH
Input capacitor ( $C_1$ )	260 $\mu$ F
Output capacitor ( $C_2$ )	260 $\mu$ F
Load (R)	120 $\Omega$
MOSFET	IRFP246
Diodes ( $D_{1,2}$ )	BYV72EW-200
Output Diode ( $D_0$ )	BYV72EW-200

## VII. FIL RESULTS.

In Fig 7, the waveforms of  $V_o$ ,  $V_{PV}$ ,  $I_o$ ,  $I_{PV}$ , and irradiance are depicted.  $I = 500 \text{ W/m}^2$ , for a given value of  $V_{PV} = 32.63 \text{ V}$ , it corresponds to a voltage  $V_o = 90.55 \text{ V}$ , let there be a voltage gain  $G = \frac{V_o}{V_{PV}} = \frac{90.55}{32.63} = 2.8$  and the duty cycle found is  $D = 0.4702$ .

The current  $I_o = 0.7546 \text{ A}$ , and  $I_{PV} = 2.277 \text{ A}$ , which results in a ratio of  $\frac{I_{PV}}{I_o} = \frac{2.277}{0.7546} = 3.017$  which is approximately equal to the voltage gain. This figure demonstrates that the output power closely follows the maximum power of the PV array, confirming the effectiveness of the developed MPPT predictive control.



(a)

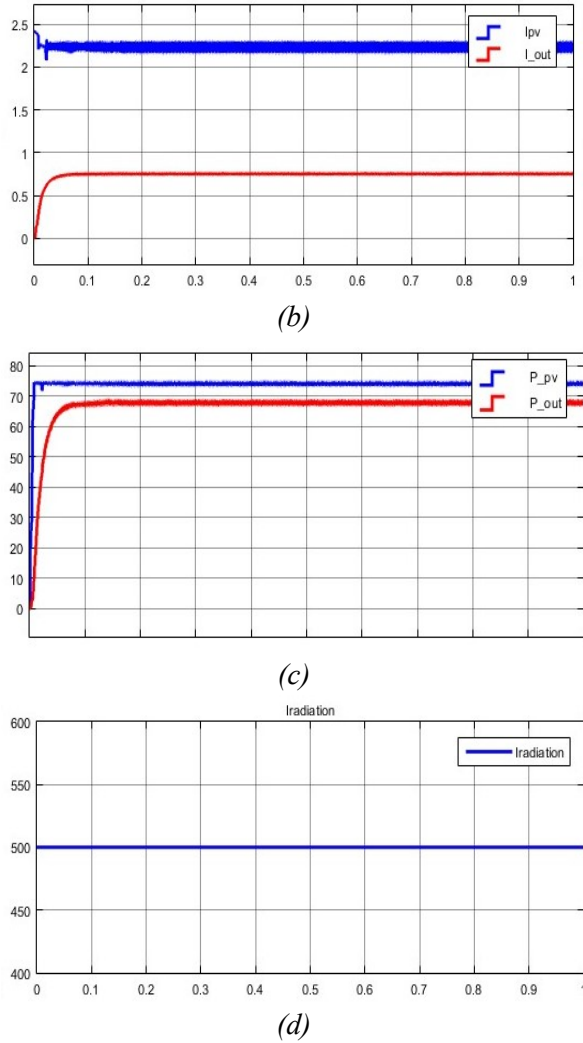
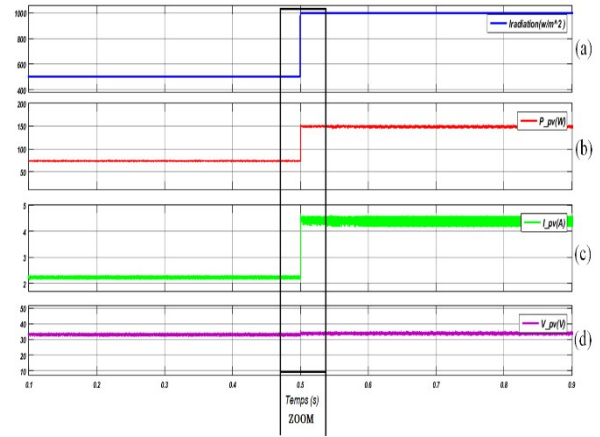


**Fig. 7.** FIL Waveforms of: (a) voltages  $V_{PV}$  and  $V_o$ , (b) currents  $I_{PV}$  and  $I_o$ , (c) powers  $P_{PV}$  and  $P_o$ , (d) irradiance  $I = 500 W/m^2$ .

Variable irradiation operation, we will observe the system's behavior during variations in irradiation. To do this, two types of profiles are considered: a step profile and a linear profile.

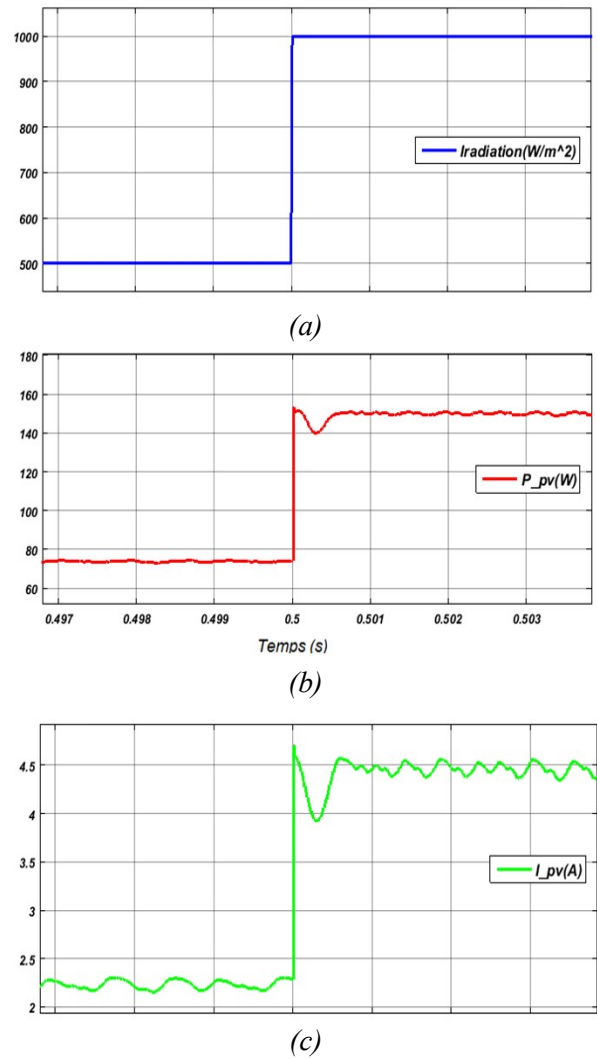
**A) Step profile**

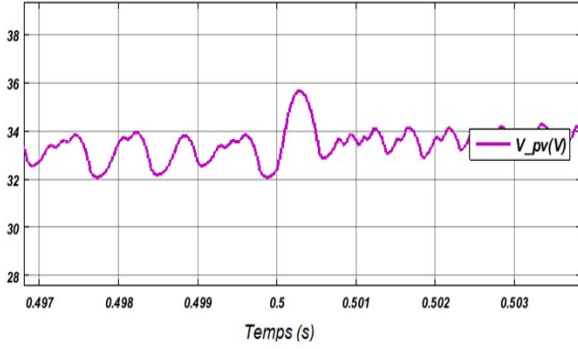
Let's consider an irradiation profile transitioning from  $500 W/m^2$  à  $1000 W/m^2$  at instant  $t = 0.5 s$  (Fig 8). the power closely follows the variations in irradiation (Fig 8.b), and the same is observed for the current  $I_{PV}$  (Fig 8.c), while  $V_{PV}$  remains nearly constant at  $32.33 V$  (Fig 8.d). This result demonstrates that irradiation affects only the current.



**Fig. 8.** FIL Waveforms of : (a) step profile of I, (b)  $P_{PV}$  power, (c)  $I_{PV}$  current, (d)  $V_{PV}$  voltage.

To better observe the system's dynamics, a zoom around the rising edge at  $t = 0.5 s$  was performed (Fig 9).





(d)

Fig. 9. FIL waveform zoom : (a) step profile of I, (b) PPV power, (c) IPV current, (d) VPV voltage.

The Fig 9.b and c demonstrate that power and current track the irradiation variation with an overshoot of approximately 3.33% and a response time of around 10 ms. As for the voltage VPV (Fig 9.d), it exhibits minimal ripples.

**B) Linear profile**

The profile adopted in this case is shown in Fig 9. irradiation linearly transitions from  $t=0.4$  s with an irradiance of  $500 \text{ W/m}^2$  to  $t = 0.7$  s with an irradiance of  $1000 \text{ W/m}^2$  (Fig 10). This figure demonstrates that power and current perfectly track the irradiation variations, while the voltage remains nearly unchanged.

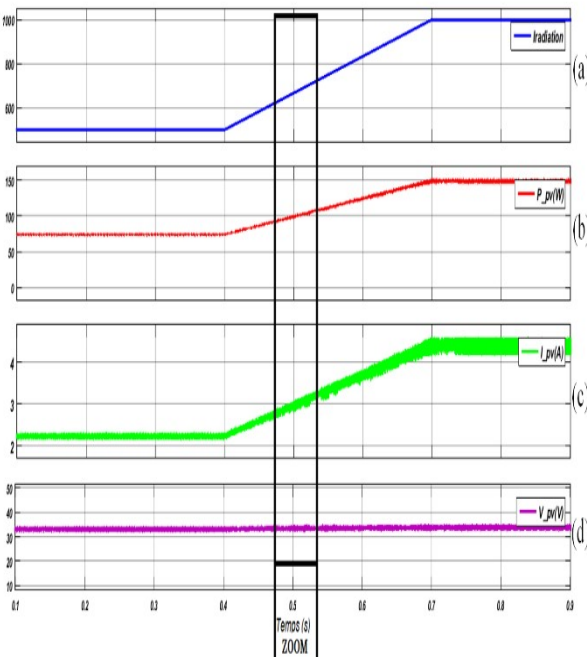
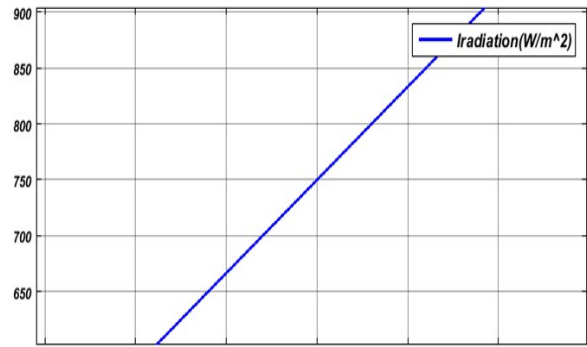


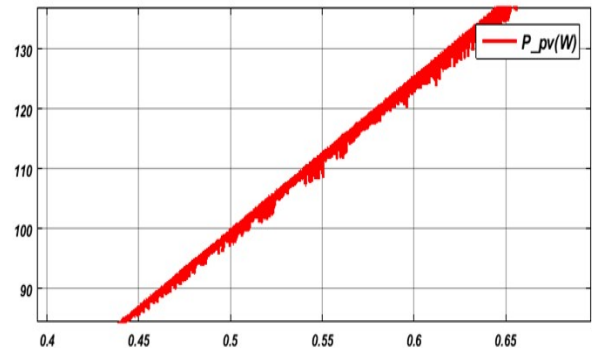
Fig. 10. FIL Waveforms of: (a) linear irradiation profile I, (b) power  $P_{PV}$ , (c) current  $I_{PV}$ , (d) voltage  $V_{PV}$ .

To observe the system's dynamics, a zoom of this fig. 10 around  $t = 0.5$  s is shown in Fig 11.

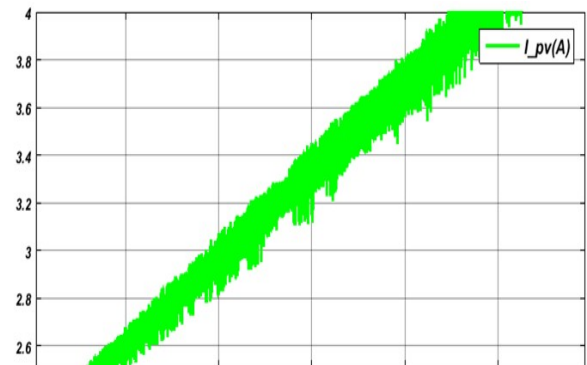
We notice that, unlike the step profile, the system for the linear profile doesn't exhibit overshoot and perfectly follows the profile (for power and current), with the voltage VPV remaining constant throughout. This profile corresponds to the real-world scenario where sunlight varies progressively. The step profile, although not representative of reality, is used to determine the system's dynamic performance in the worst-case scenario.



(a)



(b)



(c)

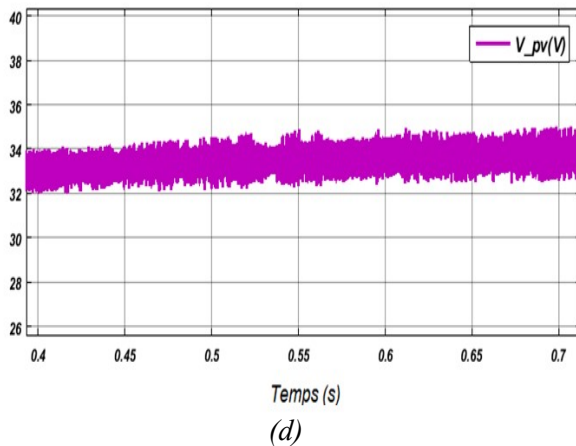


Fig. 11. FIL waveform zoom: (a) linear irradiation profile I, (b) power PPV, (c) current IPV, (d) voltage VPV.

## VIII. CONCLUSION

This paper offers a complete architecture for an FPGA based MPC-MPPT method for a high step-up DC/DC converter system for PV applications using FPGA in the Loop method. The proposed system comprised an Adaptive incremental conductance controller, and MPC controllers.

The developed MPC-MPPT algorithm, output voltage sensor has replaced by an observer to optimize the system cost and at the same time preserve the same performance. Another advantage of the developed algorithm that it could work with fixed and adaptive step-size. Although the superior performance of the proposed MPC-MPPT algorithm, working with variable switching frequency unleased the optimum design of the power converter. Both simulation and experimental results are consistence and agreed with the analytical analysis.

The whole architecture has been successfully investigated using FIL simulations on an Atlys board with spartan-6 LX45 chip. FIL results demonstrate the good operation of the suggested MPC-MPPT method.

## IX. REFERENCES

- [1] D. Divan and P. Kandula, 'Distributed power electronics: An enabler for the future grid', CPSS Trans. Power Electron. Appl., vol. 1, no. 1, pp. 57–65, Dec. 2016, doi: 10.24295/CPSSTPEA.2016.00006.
- [2] Y. Yang, A. Sangwongwanich, and F. Blaabjerg, 'Design for reliability of power electronics for grid-connected photovoltaic systems', CPSS Trans. Power Electron. Appl., vol. 1, no. 1, pp. 92–103, Dec. 2016, doi: 10.24295/CPSSTPEA.2016.00009.
- [3] 'A comprehensive review on solar PV maximum power point tracking techniques - ScienceDirect'. Accessed: Oct. 21, 2023.
- [4] A. Sangwongwanich et al., 'Enhancing PV inverter reliability with battery system control strategy', CPSS Trans. Power Electron. Appl., vol. 3, no. 2, pp. 93–101, Jun. 2018, doi: 10.24295/CPSSTPEA.2018.00009.
- [5] A. Bag, B. Subudhi, and P. K. Ray, 'An adaptive sliding mode control scheme for grid integration of a PV system', CPSS Trans. Power Electron. Appl., vol. 3, no. 4, pp. 362–371, Dec. 2018, doi: 10.24295/CPSSTPEA.2018.00035.
- [6] 'An Enhanced P&O MPPT Algorithm With Concise Search Area for Grid-Tied PV Systems | IEEE Journals & Magazine | IEEE Xplore'. Accessed: Oct. 21, 2023. [Online]. Available: <https://ieeexplore.ieee.org/abstract/document/10190565>
- [7] Q. Mei, M. Shan, L. Liu, and J. M. Guerrero, 'A Novel Improved Variable Step-Size Incremental-Resistance MPPT Method for PV Systems', IEEE Trans. Ind. Electron., vol. 58, no. 6, pp. 2427–2434, Jun. 2011, doi: 10.1109/TIE.2010.2064275.
- [8] S. C. Ferreira, R. B. Gonzatti, R. R. Pereira, C. H. da Silva, L. E. B. da Silva, and G. Lambert-Torres, 'Finite Control Set Model Predictive Control for Dynamic Reactive Power Compensation With Hybrid Active Power Filters', IEEE Trans. Ind. Electron., vol. 65, no. 3, pp. 2608–2617, Mar. 2018, doi: 10.1109/TIE.2017.2740819.
- [9] S. C. Ferreira, R. B. Gonzatti, R. R. Pereira, C. H. da Silva, L. E. B. da Silva, and G. Lambert-Torres, 'Finite Control Set Model Predictive Control for Dynamic Reactive Power Compensation With Hybrid Active Power Filters', IEEE Trans. Ind. Electron., vol. 65, no. 3, pp. 2608–2617, Mar. 2018, doi: 10.1109/TIE.2017.2740819.
- [10] [10] 'Transformerless high-gain DC–DC converter for microgrids - Revathi B. - 2016 - IET Power Electronics - Wiley Online Library'. Accessed: Oct. 21, 2023. [Online]. Available: <https://ietresearch.onlinelibrary.wiley.com/doi/full/10.1049/iet-pel.2015.0406>
- [11] M. Forouzes, Y. P. Siwakoti, S. A. Gorji, F. Blaabjerg, and B. Lehman, 'Step-Up DC–DC Converters: A Comprehensive Review of Voltage-Boosting Techniques, Topologies, and Applications', IEEE Trans. Power Electron., vol. 32, no. 12, pp. 9143–9178, Dec. 2017, doi: 10.1109/TPEL.2017.2652318.
- [12] A. D. Benhamadouche, F. Djahli, A. Ballouti, and A. Sahli, 'FPGA-based hardware-in-the-loop for multi-domain simulation', Int. J. Model. Simul. Sci. Comput., vol. 10, no. 04, p. 1950020, Aug. 2019, doi: 10.1142/S179396231950020X.
- [13] H. Bey, F. Krim, B. Talbi, and A. Sahli, 'FPGA based HIL simulation for direct current control of active power filter', in 2020 International Conference on

Electrical Engineering (ICEE), Sep. 2020, pp. 1–5. doi: 10.1109/ICEE49691.2020.9249856.

- [14] H. Bey, F. Krim, and O. Gherouat, ‘FPGA-Based Hardware in the Loop of Optimized Synergetic Controller for Active Power Filter’, *Int. Trans. Electr. Energy Syst.*, vol. 2023, p. e5810353, Mar. 2023, doi: 10.1155/2023/5810353.
- [15] O. Abdel-Rahim and H. Wang, ‘A new high gain DC-DC converter with model-predictive-control based MPPT technique for photovoltaic systems’, *CPSS Trans. Power Electron. Appl.*, vol. 5, no. 2, pp. 191–200, Jun. 2020, doi: 10.24295/CPSSPEA.2020.00016.